ELSEVIER

TiO_2 polymorphs in 'rocking-chair' Li-ion batteries

Vanchiappan Aravindan[1,*], Yun-Sung Lee[2,*], Rachid Yazami[1,3,4] and Srinivasan Madhavi[1,3,4,*]

[1] Energy Research Institute @ NTU (ERI@N), Nanyang Technological University, Research Techno Plaza, 50 Nanyang Drive, Singapore 637553, Singapore
[2] Faculty of Applied Chemical Engineering, Chonnam National University, Gwang-ju 500-757, Republic of Korea
[3] School of Materials Science and Engineering, Nanyang Technological University, Singapore 639798, Singapore
[4] TUM-CREATE, 1 Create Way, #10-02 CREATE Tower, Singapore 138602, Singapore

This review describes the overall research activities focused on developing high-performance Li-ion batteries (LIBs) fabricated with various TiO_2 polymorphs as insertion anodes. Although several polymorphs of TiO_2 have been reported, only the anatase, rutile, bronze, and brookite phases have proven promising. The bronze phase's lower insertion potential, high reversibility and high current performance makes it an attractive candidate for constructing high power and high energy density Li-ion power packs. In addition, the bronze phase exhibits superior performance over the conventional, commercialized spinel $Li_4Ti_5O_{12}$ anodes when coupled with the olivine phase $LiFePO_4$. This exceptional behavior of the bronze phase opens new avenues for the development of high power LIBs capable of powering zero emission transportation and grid storage.

Introduction

Li-ion batteries (LIBs) are one of the ubiquitous electrochemical energy storage systems of this era, known for powering numerous portable electronic appliances, toys, camcorders, laptop computers, among others. [1–3]. This diverse range of applications is primarily the result of the Li-based chemistry, which provides anodes with very low redox potential and high-potential cathodes, thereby escalating the energy density for the system. Additionally, their light-weight and long cycle-life makes them an attractive candidate for consumer electronic devices [4,5]. Recently, LIBs have been considered the most promising energy storage device for powering hybrid electric vehicles (HEVs) and electric vehicles (EVs) [6]. Therefore, a considerable amount of research has been focused on the development of LIBs with low cost and long calendar life without compromising their eco-friendliness. Commercial Li-ion cells are composed of either the olivine phase $LiFePO_4$ or a layered type $LiCoO_2$ cathode paired with graphitic anodes in the presence of aprotic solvents [7]. Unfortunately, it is not possible to use graphitic anode-based LIBs for high performance applications such as HEVs or EVs. Their potential use is hindered mainly due to unavoidable electrolyte decomposition and subsequent solid electrolyte interface (SEI) formation over the carbonaceous anodes in the first cycle, occurrence of Li-plating at high current rates, and a poor low-temperature performance. Thus, several transition metal oxide based insertion hosts, including $LiCrTiO_4$, TiP_2O_7, $LiTi_2(PO_4)_3$, $TiNb_2O_7$, Nb_2O_5, $Li_4Ti_5O_{12}$, and TiO_2, have been proposed as possible alternatives to the graphitic anodes [8–15]. While these insertion anodes have no SEI formation and an excellent high rate performance, but higher operating potential (>1.5 V *vs.* Li) and less reversible/theoretical capacity than graphitic anode remains an issue. Nevertheless, the displacement-type and alloy-based anodes exhibit a higher capacity than insertion electrodes while they experience a huge irreversible capacity loss (ICL) in the first cycle, large volume changes, higher operating potential, and poor long-term cycleability, rendering them 'show-case' materials [16–18]. Although pre-treatment of the electrodes has been proposed to suppress the ICL observed in the first cycle, the higher operating potential and long-term stability

*Corresponding authors:. Aravindan, V. (aravind_van@yahoo.com), Lee, Y.-S. (leeys@chonnam.ac.kr), Madhavi, S. (Madhavi@ntu.edu.sg)

 http://dx.doi.org/10.1016/j.mattod.2015.02.015

TABLE 1

Structural and electrochemical properties of various TiO_2 polymorphs, with their possible synthesis techniques [26].

Structure	Space group	Density (g cm^{-3})	Lattice parameter values	Lithiation quantity (mole)		Synthesis
				Bulk	Nano	
Rutile	Tetragonal $P4_2/mnm$	4.13	$a = 4.59$, $c = 2.96$	0.1	0.85	High temperature
Anatase	Tetragonal $I4_1/amd$	3.79	$a = 3.79$, $c = 9.51$	0.5	1.0	Low temperature synthesis
Brookite	Orthorhombic $Pbca$	3.99	$a = 9.17$, $b = 5.46$, $c = 5.14$	0.1	1.0	Low temperature hydrothermal
TiO_2-B (Bronze)	Monoclinic $C2/m$	3.64	$a = 12.17$, $b = 3.74$, $c = 6.51$, $\beta = 107.29^\circ$	0.71	1.0	Hydrolysis of potassium tetratitanate $K_2Ti_4O_9$, followed by heating/hydrothermal
TiO_2-II (Columbite)	Orthorhombic $Pbcn$	4.33	$a = 4.52$, $b = 5.5$, $c = 4.94$			High pressure
TiO_2-H (Hollandite)	Tetragonal $I4/m$	3.46	$a = 10.18$, $c = 2.97$			Oxidation of the related potassium titanate bronze, $K_{0.25}TiO_2$
TiO_2-III (Baddeleyite)	Monoclinic $P2_1/c$		$a = 4.64$, $b = 4.76$, $c = 4.81$, $\beta = 99.2^\circ$			High pressure
TiO_2-R (Ramsdellite)	Orthorhombic $Pbmn$	3.87	$a = 4.9$, $b = 9.46$, $c = 2.96$			Oxidation of the related lithium titanate bronze $Li_{0.5}TiO_2$
TiO_1-O I	Orthorhombic					High pressure
TiO_2-O II	Orthorhombic					$P > 40$ GPa, $T > 700^\circ$C

problems still remain unresolved [19,20]. Therefore, the only option is to develop insertion type electrodes by sacrificing the higher operating potential and have a lower practical capacity. Among the proposed insertion anodes, spinel $Li_4Ti_5O_{12}$ is appealing because of its flat operating potential at ~1.55 V *vs.* Li, no unit cell volume variation during Li-insertion/extraction (the so-called 'zero strain' insertion host), and a reversible theoretical capacity (~175 mAh g^{-1} for three moles of Li) at high current rates with appreciable coulombic efficiency; however, the capacity, unfortunately, is limited to only ~175 mAh g^{-1} [21,22]. As a result, the research focus has shifted toward developing TiO_2 polymorphs as insertion hosts for reversible accommodation of one mole Li to

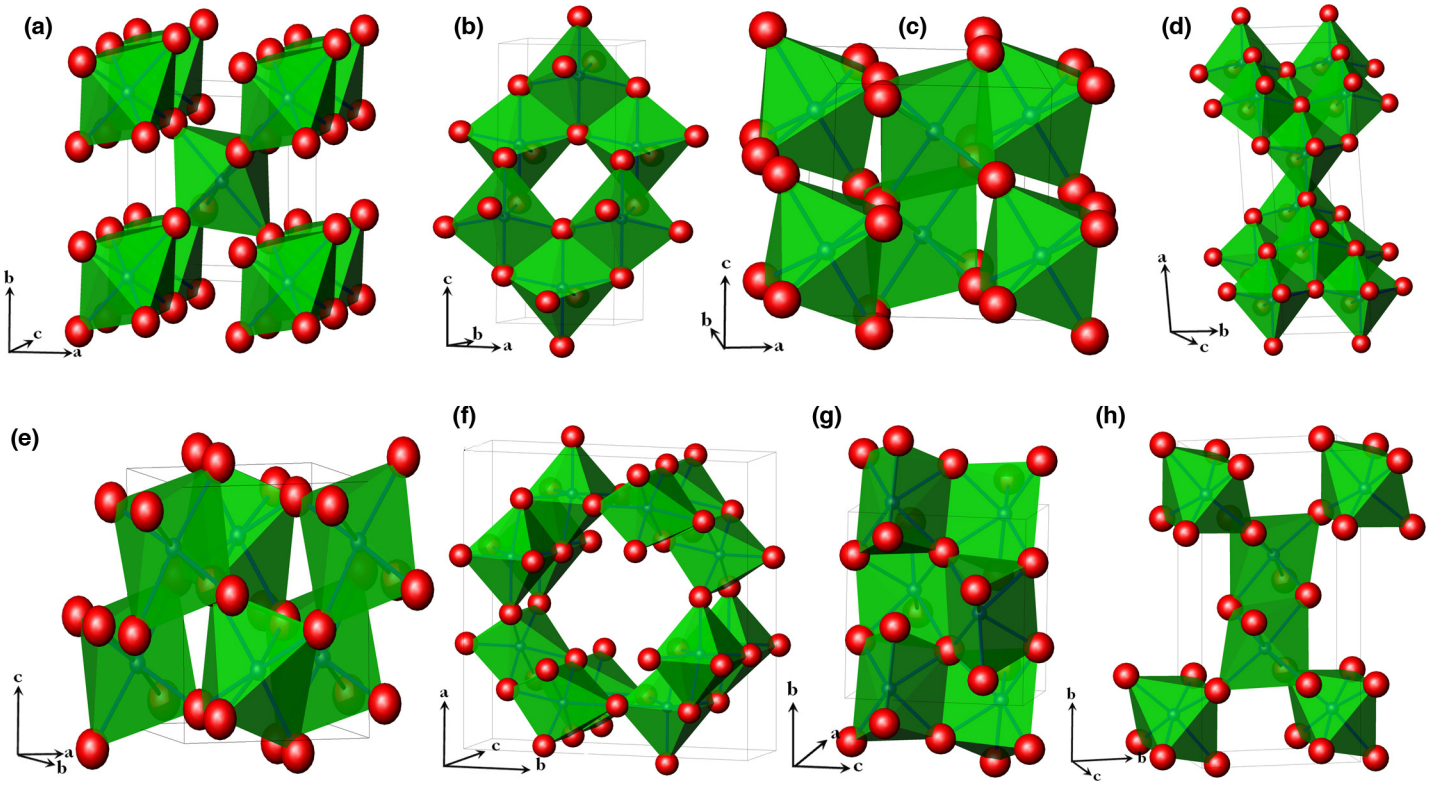

FIGURE 1

Crystal structures of (a) Rutile, (b) Anatase, (c) Bronze, (d) Brookite, (e) Columbite, (f) Hollandite, (g) Baddeleyite, and (h) Ramsdellite phases.

approach the high theoretical capacity of ~335 mAh g^{-1} [23,24]. The performances of half-cell assemblies using different TiO_2 polymorphs with varied morphological features or composites with carbon and other metal oxides have been clearly described in several reviews and original research articles [25–30]. Table 1 briefly summarizes the structural and electrochemical profiles of various TiO_2 polymorphs, and the typical crystal structures of the tabulated polymorphs are illustrated in Fig. 1. It is worth noting that several polymorphs of TiO_2 have been reported, but only a few have been explored for LIB applications, such as the anatase, rutile, brookite, and bronze phases. Amongst these, the anatase and bronze phases are electrochemically active in both the bulk and nanostructured forms with good cycleability compared to the rutile and brookite phases. Unfortunately, there are limited reports available discussing the performance of such polymorphs in a full-cell assembly (Rocking-chair configuration) with various cathode-active materials. This paper describes the recent research in implementing TiO_2 polymorphs in a full-cell assembly with conventional cathodes and its future prospects in detail.

Anatase

The anatase phase is one of the stable polymorphs that can be easily synthesized under low temperature conditions. The phase is composed of two TiO_6 octahedra sharing two adjacent edges with two other TiO_6 octahedra so that planar double chains are formed with a tetragonal body-centered space group ($I4_1/amd$) [31]. The Li diffusion in an anatase framework occurs along a reaction path connecting the octahedral interstitial sites and the diffusion coefficient (D_{Li}) values range between 1×10^{-17} and 4×10^{-17} cm^2 s^{-1} for both the Li-insertion and extraction processes. The Li insertion into an anatase lattice occurred at a relatively high potential of ~1.75 V *vs.* Li with a multi-step reaction. In general, Li insertion leads to the formation of a solid-solution (potential drop from open-circuit potential to ~1.7 V *vs.* Li) followed by a two-phase reaction (presence of a long distinct flat plateau at ~1.7 V *vs.* Li), and interfacial storage (monotonous curves beyond ~1.7 V *vs.* Li) [32–34]. However, nano-structured anatase particles also involve the formation of tetragonal phase ($LiTiO_2$) by small amount of Li-intake via Li-insertion mechanism below ~1.7 V *vs.* Li cannot be ruled out [35–39]. Exnar *et al.* [40,41] first reported on a novel ~2 V class 'rocking-chair' LIB using $LiNi_{0.5}Co_{0.5}O_2$ cathode and a nanocrystalline TiO_2 anode. The full-cell using $LiNi_{0.5}Co_{0.5}O_2/TiO_2$ delivered a reversible capacity of ~46 mAh g^{-1} (based on total mass of the electrodes) at a current density of 0.33 mA cm^{-2} with significant fading. An almost similar performance was repeated for a layered type $LiCoO_2$ cathode when coupled with the same nanocrystalline TiO_2 anode. Later, Subramanian *et al.* [42] reported on improved Li storage behavior with this type of nanocrystalline TiO_2 anode, when coupled with a $LiCoO_2$ cathode. This configuration delivered a slightly improved reversible capacity of ~95 mAh g^{-1} by tailoring the synthetic process, but the capacity fading issue remained in all the cases. A $LiCo_{1/3}Ni_{1/3}Mn_{1/3}O_2/TiO_2$ cell exhibited improved electrochemical performance than its $LiCoO_2$ and $LiNi_{0.5}Co_{0.5}O_2$ counterparts, primarily due to the 2/3 replacement of Co by Mn and Ni; however, the capacity fading remained a problem even with changing the conventional polyvinylidene fluoride (PVdF) binder to a water soluble carboxyl methyl cellulose (CMC)[43]. This clearly indicates that capacity fading is inevitable for the layered type $LiCoO_2$ and its derivatives.

The eco-friendly spinel $LiMn_2O_4$ is considered an ~4 V *vs.* Li class cathode-active material for LIB applications and is expected to replace the toxic $LiCoO_2$. Unfortunately, the Jahn-Teller distortion around the Mn^{3+} coupled with the inferior elevated-temperature performance hinders the $LiMn_2O_4$ cathode from use in commercial LIBs. Nevertheless, the ambient-temperature performance of the $LiMn_2O_4$ cathode is not inferior to that of the layered type $LiCoO_2$. Therefore, limited work has been reported on the performance of $LiMn_2O_4$ in a full-cell configuration with an anatase phase TiO_2. Kumar *et al.* [44] first reported on the performance of electrospun TiO_2 nanofibers with a commercial spinel $LiMn_2O_4$. The full-cell is capable of delivering a reversible capacity of ~104 mAh g^{-1} (based on cathode mass loading) with operating potential of ~2.1 V at current rate of 150 mA g^{-1}. However, a prominent capacity fading was also observed in the $LiMn_2O_4$/anatase TiO_2 nanofiber configuration, which reduces to ~81% of the reversible capacity after 100 cycles. Interestingly, its working potential and capacity retention is significantly better than its layered counterpart $LiCoO_2$. We believe that the capacity fading is not only associated with the synthesis of the TiO_2 nanofibers, but also with the usage of the bulk $LiMn_2O_4$ cathode which limits the Li diffusion kinetics compared to anode [45]. Hence, we successfully synthesized anatase, spinel electrodes, and PVdF-HFP membranes in one dimensional (1D) nanostructures by electrospinning [46]. The individual components were then evaluated in a half-cell assembly to examine their performance prior to LIB fabrication. As expected, the full-cell composed of all 1D components delivered exceptional performance at ~2.1 V with ~90% capacity retention after 700 cycles at ambient temperature. This extraordinary performance of all 1D nanostructures clearly suggests that the 'going-nano' concept is promising for the construction of high performance Li-ion power packs; although a small dilution in the volumetric capacity loss has to be sacrificed when comparing the cell performance, cycle life, and eco-friendliness. Xin *et al.* [47] also reported on the performance of TiO_2/graphene composite in the 18650 configuration with a $LiMn_2O_4$ cathode. Their full-cell retained ~90% (after 200 cycles) and ~80% (after 300 cycles) of its initial capacities at 1 C and 5 C rates, respectively. In both cases, the full-cell was charged using a constant current-constant voltage protocol. Unfortunately, the net operating potential was limited to ~2.1 V for the $LiMn_2O_4$/anatase TiO_2 cells, which is insufficient for high-energy applications like EVs and HEVs. Hence, research activities have increased on utilizing the $LiMn_2O_4$ derivative, $LiNi_{0.5}Mn_{1.5}O_4$, which is a well-known high voltage (~4.7 V *vs.* Li) cathode for LIB applications [48–52].

Apart from the slightly elevated operating potential (~1.75 V *vs.* Li), the ICL is another prime issue for the case of using the anatase phase. Pre-treating the electrode is one of the efficient method for ICL suppression, and this process has been successfully adopted for the fabrication of Li-ion capacitors using pre-lithiated graphitic anodes [22] and insertion electrodes for LIB applications [9,53]. Of late, Brutti *et al.* [54] introduced the concept of incorporating a small amount of nano-Li into the anatase phase to suppress the ICL observed in the first cycle. Although the ICL was suppressed after the incorporation of (2 wt.%) nano-Li, but there was an inevitable reduction in the reversible capacity compared to the

normal phase. The full-cell was fabricated with a 1.5 wt.% ZnO-modified high voltage $LiNi_{0.5}Mn_{1.5}O_4$ cathode, and the nano-Li was incorporated anatase TiO_2 as an anode. The cell displayed a reversible capacity of ~106 mAh g^{-1} (based on cathode loading) with an operating potential of ~2.8 V in line with the theoretical predictions. However, this assembly had an unexpected performance with slightly inferior coulombic efficiency (~95%) and severe capacity fading (the ZnO-modified $LiNi_{0.5}Mn_{1.5}O_4$/nano-Li incorporated TiO_2 cell retained only ~75% of its initial capacity after 50 cycles). Later, Plylahan *et al.* [55] reported the fabrication of self-supported TiO_2 nanotubes with $LiNi_{0.5}Mn_{1.5}O_4$ in the presence of a dry solid polymer electrolyte, $LiN(CF_3SO_2)_2$, (LiTFSI) in methyl methacrylate-polyethylene oxide, MMA-PEO. Although the full-cell delivered excellent cycling profiles (~92% capacity retention after 100 cycles), the reported operating potential (~2.2 V) was much lower than the predicted value (~2.8 V). Very recently, Arun *et al.* [56] successfully repeated the concept of fabricating a LIB using the 1D nanostructures reported by Aravindan *et al.* [46] with a high voltage spinel $LiNi_{0.5}Mn_{1.5}O_4$. The fabrication process of the electrospun $LiNi_{0.5}Mn_{1.5}O_4$ nanofiber assembly was similar to all 1D hollow structured systems ($LiMn_2O_4$/PVdF-HFP/TiO_2), but the morphologies were slightly different. As expected, there was no severe capacity fading observed in all 1D full-cell, $LiNi_{0.5}Mn_{1.5}O_4$/PVdF-HFP/TiO_2, compared to the pre-treated TiO_2 based configuration [54]. Here, the ICL observed in the anatase phase was addressed by adding slightly more than the estimated cathode-active material loading (e.g., 5 wt.%). In addition to this high voltage configuration, all full-cell assemblies based on the anatase TiO_2 anode reported by Aravindan *et al.* [44,46,57] followed the same strategy. As a result, excellent electrochemical cycling profiles were achieved. The full-cell retained ~86% of its initial reversible capacity after 400 cycles at a 2 C rate (2 C = 300 mAh g^{-1}), which is superior to that reported by Brutti *et al.* [54] for the nano-Li incorporated anatase phase. Nonetheless, the capacity fading is slightly higher for the $LiNi_{0.5}Mn_{1.5}O_4$ compared to its native phase ($LiMn_2O_4$) when coupled with an anatase phase, primarily due to the existence of a high voltage $Ni^{2+/4+}$ redox couple (~4.7 V *vs.* Li) falling at a slightly higher potential than the decomposition potential of conventional carbonate-based electrolyte solutions [7]. This high voltage configuration clearly parallels and validates the advantages of 'going-nano' concept for the fabrication of high performance LIBs.

$LiFePO_4$ is one of the promising cathode materials for LIB applications, as it has an operating potential of ~3.4 V *vs.* Li. The electrochemical activity of olivine $LiFePO_4$ was first reported by Goodenough *et al.* [58] in 1997 and recently commercialized with graphitic anodes by several companies, such as Sony and K2 energy. Further, high theoretical capacity (170 mAh g^{-1}), good cycle-life, appreciable redox potential (~3.4 V *vs.* Li) located in the electrochemically stable window of conventional carbonate-based electrolytes, flat charge-discharge profile, ability to sustain high current rates, natural abundance, low-cost, eco-friendliness and thermal and chemical stability are also worth a mention for olivine phase $LiFePO_4$ cathode. Taking the advantages of the olivine phase cathode, the full-cell was fabricated with an anatase phase TiO_2. It is unfortunate that the slightly lower redox couple of $Fe^{2+/3+}$ translate to a theoretical net operating potential of ~1.7 V. Choi *et al.* [59,60] first reported on the assembly and performance of a $LiFePO_4$/TiO_2-graphene composite. Their full-cell delivered a reversible capacity of ~125 mAh g^{-1} (based on cathode mass loading) at a 1 C rate (1 C = 170 mAh g^{-1}) with a flat operating potential of ~1.4 V. However, this assembly's net operating potential was slightly lower than the predicted potential (~1.65 V). By contrast, an excellent cycleability of 700 cycles was noted for this $LiFePO_4$/TiO_2-graphene composite cell under ambient conditions. A similar result was reported by Zhang *et al.* [57] where the full-cell was composed of TiO_2 nanofibers prepared by co-axial electrospinning. The electrospun fibers delivered an excellent performance in a half-cell assembly (Li/TiO_2 nanofibers), for example, ~84% of its initial reversible capacity was retained after 300 cycles at a current density of 100 mA g^{-1} (based on cathode mass loading). Hence, the same performance was anticipated in the full-cell configuration. In the full-cell, the $LiFePO_4$/TiO_2 nanofibers delivered a capacity of ~103 mAh g^{-1} with an operating potential of ~1.4 V, and retained ~88% of its initial reversible capacity after 300 cycles. Compatibility with the water soluble binder, CMC, in the full-cell assembly ($LiFePO_4$ cathode) also reported by Mancini *et al.* [61] with a good cycleability of 50 cycles, a designed capacity of ~780 mAh, and at a 1 C rate. A mesoporous carbon-coated TiO_2 nanosphere was synthesized via a hydrothermal approach reported by Cao *et al.* [62]. In the half-cell assembly, the carbon-coated TiO_2 nanospheres delivered a capacity of ~185 mAh g^{-1} at a 0.2 C rate with reasonable cycleability. However, in the full-cell assembly, an unusual increase in the mass loading of the anode side was noted. As a result, the net operating potential increased to over ~1.5 V when coupled with the olivine $LiFePO_4$. Unfortunately, there was no extended cycling reported for this configuration. Figure 2 displays typical electrochemical performances of anatase phase anodes in full-cell assemblies with various eco-friendly cathodes, including $LiFePO_4$, $LiMn_2O_4$, and $LiNi_{0.5}Mn_{1.5}O_4$.

Bronze

The Li insertion into anatase TiO_2 is a multi-step process, including a solid-solution formation, a two-phase reaction, a bulk-intercalation, and interfacial storage. Nevertheless, the TiO_2-bronze (B) phase has emerged as a prospective candidate owing to its salient features, such as a lower operating potential (~1.55 *vs.* Li) compared to the anatase phase (~1.75 *vs.* Li), a considerably improved reversibility (only ~0.5 of Li is reversible in the anatase phase), and a high power capability [63,64]. Furthermore, unlike the anatase phase, there is no complicated Li insertion reaction mechanism noted for the bronze phase due to its relatively more open crystal structure [65]. This type of structure is ideal for the facile insertion/extraction of Li ions, and it additionally displays a *n*-type electronic conductivity. Bruce *et al.* [66,67] reported on the performance of TiO_2-B anodes with two cathodes: olivine $LiFePO_4$ and the high voltage spinel $LiNi_{0.5}Mn_{1.5}O_4$ in the presence of a gel polymer electrolyte ($LiPF_6$ trapped in EC-PC-PVdF). Theoretically, the $LiFePO_4$/TiO_2-B and $LiNi_{0.5}Mn_{1.5}O_4$/TiO_2-B configurations are able to operate at ~1.9 and ~3.15 V, respectively. Interestingly, the energy density of the $LiFePO_4$/TiO_2-B assembly was nearly identical to that of the toxic layered $LiCoO_2$ (and its derivatives)/anatase TiO_2 configuration. Both the olivine and spinel based configuration delivered

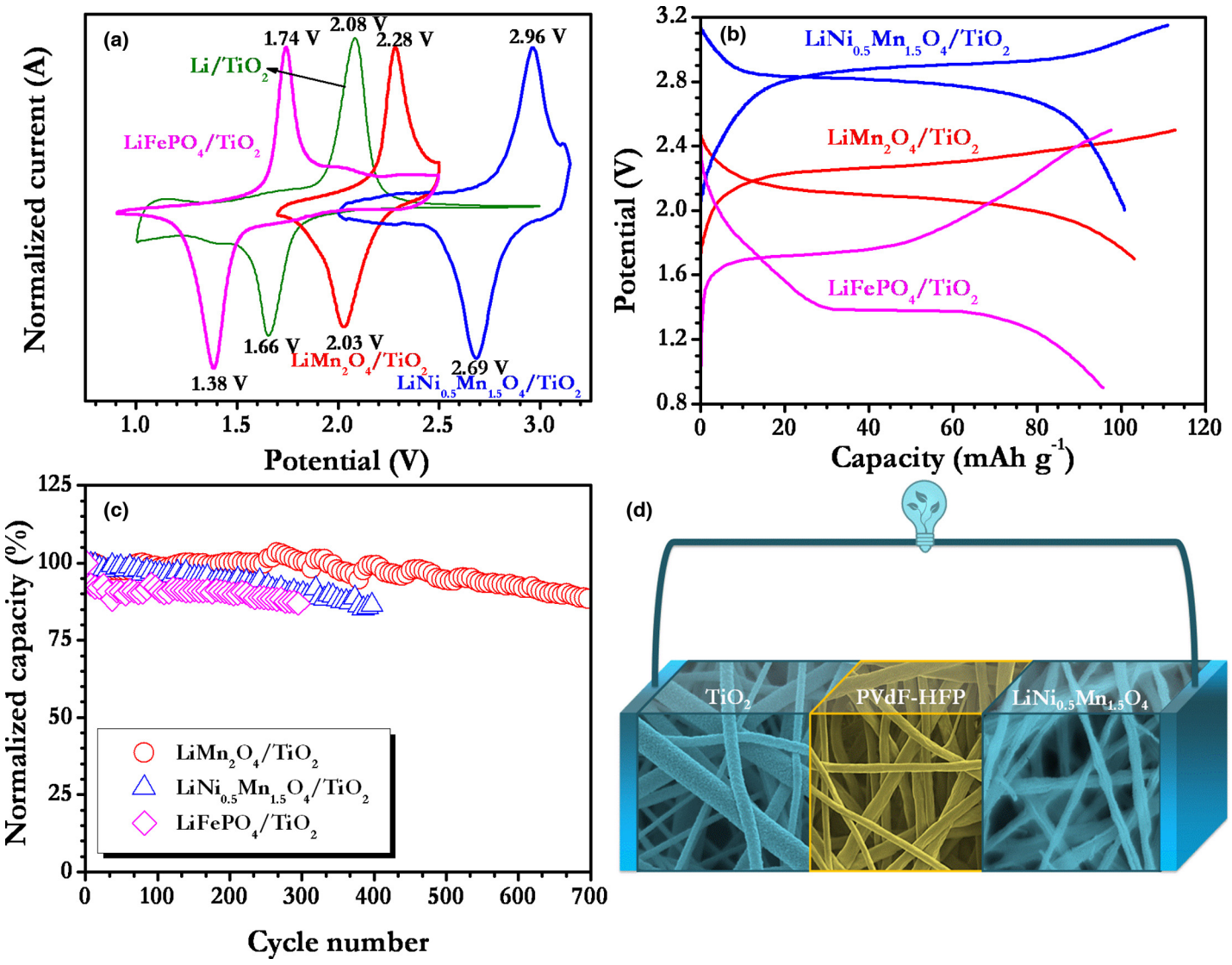

FIGURE 2

(a) Typical CV signatures of anatase TiO_2 anodes in full-cell assemblies with eco-friendly cathodes: $LiMn_2O_4$ (red line), $LiNi_{0.5}Mn_{1.5}O_4$ (blue line), and $LiFePO_4$ (pink line) at a slow 0.1 mV s^{-1} scan rate. The performance of anatase TiO_2 in a half-cell assembly (Li/TiO_2) is also given (green dashed line) for comparison. (b) Typical galvanostatic charge-discharge curves of $LiMn_2O_4/TiO_2$ (red line, current density: 150 mA g^{-1}), $LiNi_{0.5}Mn_{1.5}O_4/TiO_2$ (blue line, current density: 15 mA g^{-1}), and $LiFePO_4/TiO_2$ (pink line, current density: 100 mA g^{-1}) cells. (c) Plot of the normalized reversible capacity of the aforementioned cells relative to the number of cycles. (d) Schematic representation of a typical LIB composed of all 1D-nanostructured components. Reproduced from Ref. [46,56,57] with permission from The Royal Society of Chemistry.

a reversible capacity of ~225 mAh g^{-1} (based on anode mass loading) and an excellent cycleability with a coulombic efficiency over 99%. This ensures a reproducibility and compatibility with various insertion cathodes. Interestingly, the performance of the $LiFePO_4/TiO_2$-B compared to the $LiFePO_4/Li_4Ti_5O_{12}$ found that the former exhibited a significantly better reversible capacity, energy density, and rate capability over the latter. Recently, Guo *et al.* [68] reported a detailed investigation on both the $LiFePO_4/TiO_2$-B and $LiFePO_4/Li_4Ti_5O_{12}$ systems. Among these, the former exhibited a significantly improved energy density, durability (300 cycles), and rate capability than the latter. The $LiFePO_4/TiO_2$-B cell retained ~70% of its initial reversible capacity after 300 cycles at a current density of 4 A g^{-1} (based on anode mass loading). Although a high power capability is achieved for this bronze phase TiO_2 when coupled with the olivine phase $LiFePO_4$, the energy density remains an issue for such assemblies. In this regard, Aravindan *et al.* [32] reported an excellent performance of hydrothermally prepared TiO_2-B nanorods with a spinel $LiMn_2O_4$ cathode. The cycling profiles of these $LiMn_2O_4/TiO_2$-B cells were compared with a Whatman separator and an electrospun PVdF-HFP nanofiber membrane for approximately 1000 cycles at a 150 mA g^{-1} current density under ambient conditions. After 1000 cycles, the $LiMn_2O_4/TiO_2$-B nanorods showed capacity retentions of ~74 and ~67% for the Whatman separator and electrospun PVdF-HFP membranes, respectively. Moreover, the full-cell displayed an ~120 mAh g^{-1} reversible capacity and ~2.5 V operating potential. Figure 3 shows the typical electrochemical performances of bronze phase anodes with $LiFePO_4$ and $LiMn_2O_4$ cathodes (for both the Whatman and electrospun PVdF-HFP separators).

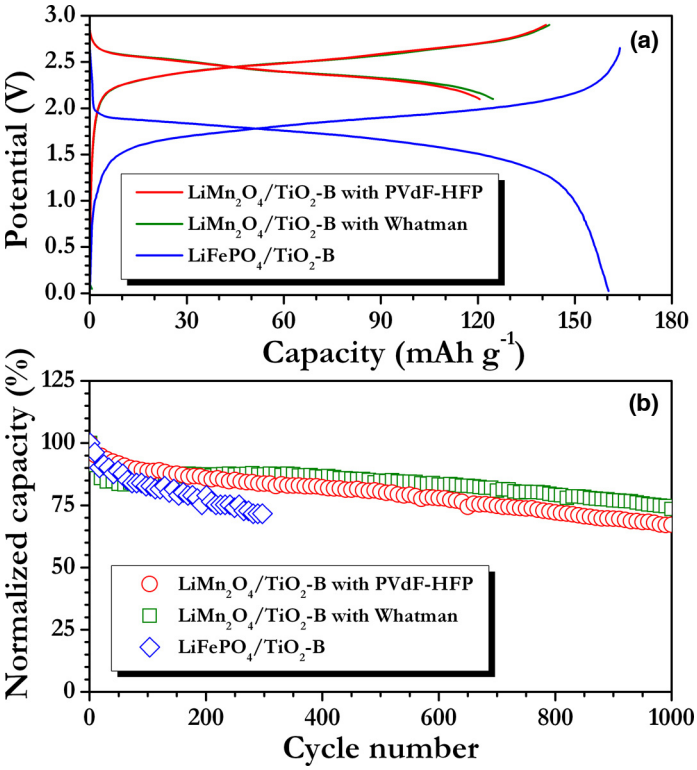

FIGURE 3

(a) Typical charge-discharge curves of $LiMn_2O_4/TiO_2$-B cells with Whatman (green line) or PVdF-HFP (red line) separators at a 150 mA g^{-1} current density, and $LiFePO_4/TiO_2$-B (blue line) (capacity calculated based on anode active mass). (b) Plot of the normalized reversible capacity *vs.* cycle number for $LiMn_2O_4/TiO_2$-B cells at a 150 mA g^{-1} current density with Whatman (green squares) or PVdF-HFP (red circles) separators, and $LiFePO_4/TiO_2$-B (blue diamonds) at a 4 A g^{-1} current density (for this measurement the cell was charged to 2.65 V with a 4 A g^{-1} current density, and the battery voltage was held at 2.65 V for 1 min, that is, constant current-constant voltage mode). Reproduced from Ref. [32,68] with permission from The Royal Society of Chemistry.

Rutile

Unlike the anatase and bronze phases, the rutile phase is one of the more stable polymorphs, but it has not been explored in depth because of its inferior electrochemical activity toward Li in both the nanoscale and bulk form. In its bulk crystalline form, it can accommodate up to 0.1 mole of Li, whereas at elevated temperatures (e.g., 120°C), the intake level improved to 0.5 mole of Li. It is well known that the Li diffusion in the rutile phase is highly anisotropic, proceeding through rapid diffusion along *c*-axis channels. The Li^+ diffusion coefficient along the *c*-axis was found to be $\sim 10^{-6}$ cm^2 s^{-1}, whereas in the *ab*-plane it is only approximately 10^{-15} cm^2 s^{-1} [69]. As a result, the Li migration and desirable filling of octahedral sites are highly limited by the *c*-channels. In addition, the strong repulsive Li–Li interactions in the *c*-channels together with trapped Li ion pairs in the *ab*-planes may block the *c*-channels, restricting insertion to well below its theoretical limit. Particulate size is reduced to below 10 nm results the accommodation of ~0.85 mole of Li. The Li-insertion reaction progressed through two solid solution domains, and then via the irreversible phase transformation of electro-active $LiTiO_2$ (rock-salt type) because of the expansion of *ab*-plane [70]. As a consequence, 0.5 mole of Li is reversibly cycled with good stability which is similar to the reversibility of bulk anatase phase. By

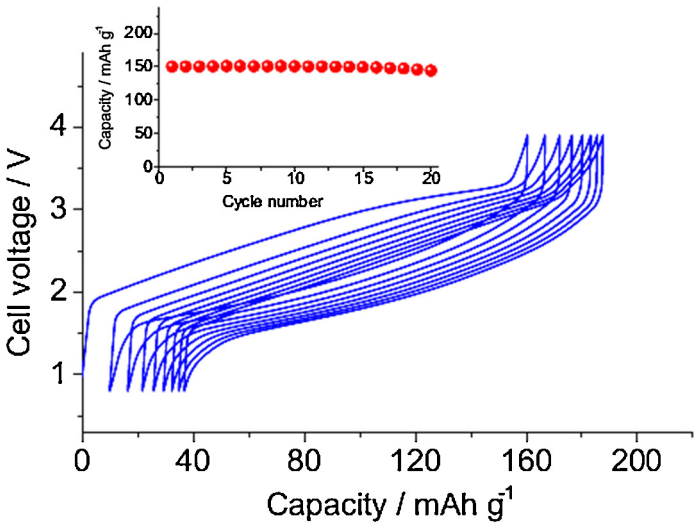

FIGURE 4

Voltage profile and inset cycling behavior of the galvanostatic test performed on the $LiFePO_4/TiO_2$ lithium ion cell performed at C/3 rate (1 C = 170 mA g^{-1}) in the 0.8–3.8 V voltage range. EC:DMC 1:1, $LiPF_6$ 1 M electrolyte. Room Temperature. Reproduced from Ref. [73] with permission from Elsevier.

contrast, Hu *et al.* [71] suggests that the surface storage is more favorable for rutile phase compared to the bulk intercalation. However, Wohlfahrt-Mehrens *et al.* [72] recently reported on the electrochemical Li insertion properties in nanoscale rutile particulates. Later, Hassoun *et al.* [73] repeated their synthesis procedure to construct a full-cell assembly using the TiO_2 rutile phase (crystallite size of 10 nm) as anode and the olivine $LiFePO_4$ as cathode. The full-cell delivered a reversible capacity of ~150 mAh g^{-1} with appreciable cycleability for 20 cycles between 0.8 and 3.8 V under ambient conditions. By contrast, a poor high-temperature (90°C) performance was noted for this configuration. In the high temperature tests, the conventional liquid electrolyte (1 M $LiPF_6$ in EC:DMC) was replaced with a composite solid polymer electrolyte ((polyethylene oxide)$_{20}LiCF_3SO_3$ + 10 wt.% ZrO_2) to retain cell stability (Fig. 4). Unexpectedly, a reversible capacity of ~75 mAh g^{-1} was only obtained after 40 cycles in the high temperature conditions, mainly resulting from the unbalanced mass loading of the electrodes.

Summary and outlook

Although the existence of several polymorphs has been reported for TiO_2, very few, including the anatase, rutile, brookite, and bronze phases, have been investigated as insertion anodes for LIB applications. Among the polymorphs investigated, a severe capacity fading was noted for the brookite phase in a half-cell configuration, although it exhibited nearly one mole of reversible Li insertion/extraction in its nanostructured form [74–76]. Hence, there has not been extensive research focused on developing such an anode. Similar to brookite, the rutile phase has also been eliminated from practical applications because of its inferior electrochemical activity; nevertheless, Hassoun *et al.*'s [73] work is an exception. However, further research is underway to improve the electrochemical activity of both the brookite and rutile phases. Both the anatase and bronze phases in their nanostructured forms are under extensive investigation as promising insertion anodes with varied morphological features, and as composites with several carbonaceous allotropes. However, the electrochemical Li

insertion properties of the anatase and bronze phases were found to be entirely different from one another. Amongst these, the bronze phase was found to be superior due to its lower operating potential, higher reversibility, and high power capability over the anatase phase. In addition, the bronze phase exhibited more favorable electrochemical properties than the conventional spinel $Li_4Ti_5O_{12}$ anode, which has been clearly supported by Armstrong *et al.*'s [66] and Guo *et al.*'s [68] works with the olivine phase $LiFePO_4$ cathode, particularly at high current operations. Additionally, the bronze phase delivered an exceptional cycleability over 1000 cycles when coupled with a spinel $LiMn_2O_4$ cathode, irrespective of the type of separator used (Whatman or electrospun PVdF-HFP membrane). By contrast, apart from the academic interest, there is no scope for the development of anatase phase-based Li-ion cells for practical applications, due to its poor rate performance and reversibility (only 0.5 mole of Li is reversible), notable ICL in the first cycle, and higher operating potential than the bronze phase. The poor rate performance can be circumvented by adding this phase to a carbon matrix or as part of a composite, but latter two issues remain. However, we strongly believe the exceptional performances of the bronze phase at high current rates are mainly attributed to its crystal structure, apart from the nanostructured form. The monoclinic TiO_2-B is composed of edge and corner sharing TiO_6 octahedral units, with the corrugated sheets joined together to form a three-dimensional framework [77]. This kind of open framework structure is beneficial for the facile diffusion of Li-ions. As a result, a high energy and high power Li-ion battery can be fabricated using the bronze phase anode with high voltage cathodes, fulfilling the necessary requirements to drive zero emission transportation, such as EVs and HEVs. Unfortunately, the meager capacity fading in both the half-cell and full-cell assemblies is an important issue hindering the usage of bronze phase, and must be addressed before reaching commercial applications, which will most likely be in the production of composites with carbonaceous materials, among others. Additionally, it should be noted that the fabrication of Li-ion cells using all 1D nanostructured components displayed exceptional performance irrespective of the cathode or anode used. Studies must also focus on investigating the performance of this bronze phase in an all 1D assembly. Therefore, we strongly believe the bronze phase is one of the most important and promising insertion hosts among the TiO_2 polymorphs, and remains a strong competitor for the development of high power and high energy density Li-ion power packs compared to conventional spinel phase $Li_4Ti_5O_{12}$.

Acknowledgements

This work was financially supported by the Singapore National Research Foundation under its Campus for Research Excellence And Technological Enterprise (CREATE) program. YSL acknowledge the financial support from the Energy Efficiency and Resources R&D program (20112010100150) under the Ministry of Knowledge Economy, Republic of Korea. Authors wishes to thank Dr Tom Baikie for his help toward making the crystal structures.

References

[1] V. Aravindan, et al. J. Mater. Chem. A 1 (11) (2013) 3518.
[2] H.D. Yoo, et al. Mater. Today 17 (3) (2014) 110.
[3] E.M. Erickson, et al. J. Phys. Chem. Lett. 5 (19) (2014) 3313.
[4] M. Armand, J.-M. Tarascon, Nature 451 (7179) (2008) 652.
[5] V. Aravindan, et al. Chem. Asian. J. 9 (3) (2014) 878.
[6] O.K. Park, et al. Energy Environ. Sci. 4 (5) (2011) 1621.
[7] V. Aravindan, et al. Chem. Asian. J. 17 (51) (2011) 14326.
[8] V. Aravindan, et al. Chem. Rev. 114 (23) (2014) 11619.
[9] R. Satish, et al. Adv. Energy Mater. 4 (9) (2014) 1301715.
[10] S. Jayaraman, et al. ACS Appl. Mater. Interfaces 6 (11) (2014) 8660.
[11] L.H. Nguyen, et al. ChemElectroChem 1 (3) (2014) 539.
[12] V. Aravindan, et al. ChemSusChem 7 (7) (2014) 1858.
[13] J. Sundaramurthy, et al. J. Phys. Chem. C 118 (30) (2014) 16776.
[14] V. Aravindan, et al. Chem. Commun. 51 (12) (2015) 2225.
[15] M.V. Reddy, et al. Chem. Rev. 113 (7) (2013) 5364.
[16] N.-S. Choi, et al. Angew. Chem. Int. Ed. 51 (40) (2012) 9994.
[17] Y. Idota, et al. Science 276 (5317) (1997) 1395.
[18] P. Poizot, et al. Nature 407 (6803) (2000) 496.
[19] A. Varzi, et al. Adv. Energy Mater. 4 (10) (2014) 1400054.
[20] R. Verrelli, et al. J. Mater. Chem. A 1 (48) (2013) 15329.
[21] K. Naoi, et al. Acc. Chem. Res. 46 (5) (2013) 1075.
[22] K. Naoi, et al. Energy Environ. Sci. 5 (11) (2012) 9363.
[23] D. Deng, et al. Energy Environ. Sci. 2 (8) (2009) 818.
[24] Z. Chen, et al. Adv. Funct. Mater. 23 (8) (2013) 959.
[25] L. Kavan, J. Solid State Electrochem. 18 (8) (2014) 2297.
[26] Z. Liu, et al. Prog. Nat. Sci.: Mater. Int. 23 (3) (2013) 235.
[27] L. Kavan, Chem. Rec. 12 (1) (2012) 131.
[28] A.G. Dylla, et al. Acc. Chem. Res. 46 (5) (2013) 1104.
[29] Z. Yang, et al. J. Power Sour. 192 (2) (2009) 588.
[30] M. Koudriachova, J. Solid State Electrochem. 14 (4) (2010) 549.
[31] G.F. Ortiz, et al. Chem. Mater. 21 (1) (2008) 63.
[32] V. Aravindan, et al. J. Mater. Chem. A 1 (2) (2013) 308.
[33] V. Aravindan, et al. J. Mater. Chem. A 1 (20) (2013) 6145.
[34] Y.G. Guo, et al. Adv. Mater. 19 (16) (2007) 2087.
[35] J.-Y. Shin, et al. Adv. Funct. Mater. 21 (18) (2011) 3464.
[36] W.J.H. Borghols, et al. J. Am. Chem. Soc. 131 (49) (2009) 17786.
[37] V. Gentili, et al. Chem. Mater. 24 (22) (2012) 4468.
[38] M. Wagemaker, et al. J. Am. Chem. Soc. 129 (14) (2007) 4323.
[39] M. Wagemaker, et al. Chem. Eur. J. 13 (7) (2007) 2023.
[40] I. Exnar, et al. J. Power Sour. 68 (2) (1997) 720.
[41] S.Y. Huang, et al. J. Electrochem. Soc. 142 (9) (1995) L142.
[42] V. Subramanian, et al. J. Power Sour. 159 (1) (2006) 186.
[43] A. Moretti, et al. J. Power Sour. 221 (0) (2013) 419.
[44] P. Suresh Kumar, et al. RSC Adv. 2 (21) (2012) 7983.
[45] S. Jayaraman, et al. Chem. Commun. 49 (59) (2013) 6677.
[46] V. Aravindan, et al. Nanoscale 5 (21) (2013) 10636.
[47] X. Xin, et al. ACS Nano 6 (12) (2012) 11035.
[48] M.C. Kim, et al. ChemSusChem 7 (3) (2014) 829.
[49] W.H. Jang, et al. Electrochim. Acta 137 (0) (2014) 404.
[50] W.H. Jang, et al. J. Alloys Compd. 612 (0) (2014) 51.
[51] M.C. Kim, et al. J. Electrochem. Soc. 160 (8) (2013) A1003.
[52] A. Manthiram, et al. Energy Environ. Sci. 7 (4) (2014) 1339.
[53] Y.L. Cheah, et al. ACS Appl. Mater. Interfaces 5 (8) (2013) 3475.
[54] S. Brutti, et al. J. Power Sour. 196 (22) (2011) 9792.
[55] N. Plylahan, et al. Electrochem. Commun. 43 (2014) 121.
[56] N. Arun, et al. Nanoscale 6 (15) (2014) 8926.
[57] X. Zhang, et al. Nanoscale 5 (13) (2013) 5973.
[58] A.K. Padhi, et al. J. Electrochem. Soc. 144 (4) (1997) 1188.
[59] D. Choi, et al. Electrochem. Commun. 12 (3) (2010) 378.
[60] T. Xu, et al. J. Manage. 62 (9) (2010) 24.
[61] M. Mancini, et al. J. Power Sour. 196 (22) (2011) 9665.
[62] F.-F. Cao, et al. J. Phys. Chem. C 114 (22) (2010) 10308.
[63] Y. Ren, et al. Angew. Chem. Int. Ed. 51 (9) (2012) 2164.
[64] A.R. Armstrong, et al. J. Power Sour. 146 (1–2) (2005) 501.
[65] T.P. Feist, P.K. Davies, J. Solid State Chem. 101 (2) (1992) 275.
[66] G. Armstrong, et al. Adv. Mater. 18 (19) (2006) 2597.
[67] P.G. Bruce, Solid State Ionics 179 (21–26) (2008) 752.
[68] Z. Guo, et al. RSC Adv. 3 (10) (2013) 3352.
[69] M. Pfanzelt, et al. J. Power Sour. 196 (16) (2011) 6815.
[70] E. Baudrin, et al. Electrochem. Commun. 9 (2) (2007) 337.
[71] Y.S. Hu, et al. Adv. Mater. 18 (11) (2006) 1421.
[72] P. Kubiak, et al. J. Power Sour. 194 (2) (2009) 1099.
[73] J. Hassoun, et al. J. Power Sour. 217 (0) (2012) 459.
[74] M. Anji Reddy, et al. Electrochem. Solid State Lett. 11 (8) (2008) A132.
[75] M.A. Reddy, et al. Electrochem. Solid State Lett. 10 (2) (2007) A29.
[76] D.W. Murphy, et al. Solid State Ionics 9–10, Part 1 (0) (1983) 413.
[77] Y.G. Andreev, et al. J. Am. Chem. Soc. 136 (17) (2014) 6306.